

Autocatalytic Cycles in a Copper-Catalyzed Azide-Alkyne Cycloaddition Reaction

Sergey N Semenov, Lee Belding, Brian J. Cafferty, Maral P. S. Mousavi, Anastasiia M. Finogenova, Ricardo S. Cruz, Ekaterina V. Skorb, and George M. Whitesides

J. Am. Chem. Soc., **Just Accepted Manuscript** • DOI: 10.1021/jacs.8b05048 • Publication Date (Web): 23 Jul 2018

Downloaded from <http://pubs.acs.org> on July 23, 2018

Just Accepted

“Just Accepted” manuscripts have been peer-reviewed and accepted for publication. They are posted online prior to technical editing, formatting for publication and author proofing. The American Chemical Society provides “Just Accepted” as a service to the research community to expedite the dissemination of scientific material as soon as possible after acceptance. “Just Accepted” manuscripts appear in full in PDF format accompanied by an HTML abstract. “Just Accepted” manuscripts have been fully peer reviewed, but should not be considered the official version of record. They are citable by the Digital Object Identifier (DOI®). “Just Accepted” is an optional service offered to authors. Therefore, the “Just Accepted” Web site may not include all articles that will be published in the journal. After a manuscript is technically edited and formatted, it will be removed from the “Just Accepted” Web site and published as an ASAP article. Note that technical editing may introduce minor changes to the manuscript text and/or graphics which could affect content, and all legal disclaimers and ethical guidelines that apply to the journal pertain. ACS cannot be held responsible for errors or consequences arising from the use of information contained in these “Just Accepted” manuscripts.



Autocatalytic Cycles in a Copper-Catalyzed Azide-Alkyne Cycloaddition Reaction

Sergey N. Semenov,^{a,‡} Lee Belding,^a Brian J. Cafferty,^a Maral P.S. Mousavi,^a Anastasiia M. Finogenova,^a Ricardo S. Cruz,^a Ekaterina V. Skorb,^{a,†} and George M. Whitesides^{a,b,c,*}

^a *Department of Chemistry and Chemical Biology, Harvard University*

12 Oxford Street, MA 02138

^b *Kavli Institute for Bionano Inspired Science and Technology, School of Engineering and Applied Sciences, Harvard University*

29 Oxford Street, MA 02138

^c *Wyss Institute for Biologically Inspired Engineering, Harvard University*

60 Oxford Street, MA 02138

* Author to whom correspondence should be addressed.

Abstract

This work describes the autocatalytic copper-catalyzed azide-alkyne cycloaddition (CuAAC) reaction between tripropargylamine and 2-azidoethanol, in the presence of Cu(II) salts. The product of this reaction, *tris*-(hydroxyethyltriazolylmethyl)amine ($\text{N}(\text{C}_3\text{N}_3)_3$), accelerates the cycloaddition reaction (and thus its own production) by two mechanisms: i) by coordinating Cu(II) and promoting its reduction to Cu(I), and ii) by enhancing the catalytic reactivity of Cu(I) in the cycloaddition step. Because of the cooperation of these two processes, a rate enhancement of > 400x is observed over the course of the reaction. The kinetic profile of the autocatalysis can be controlled by using different azides and alkynes, or ligands (*e.g.*, ammonia) for Cu(II). When carried out in a layer of 1% agarose gel, and initiated by ascorbic acid, this autocatalytic reaction generates an autocatalytic front. This system is prototypical of autocatalytic reactions where the formation of a product, which acts as a ligand for a catalytic metal ion, enhances the production and activity of the catalyst.

Introduction

Autoamplification and autocatalysis are important – although surprisingly uncommon – types of processes in chemistry.¹ Biological cellular division is – in a sense – a type of autoamplification. Flames and explosions are autocatalytic, as is the formose reaction,²⁻³ silver-halide photography,⁴ photolithography using chemically amplified photoresists,⁵⁻⁷ crystallization, electroless deposition of metals,⁸ the Soai reaction,⁹⁻¹² the formaldehyde–sulfite reaction,¹³⁻¹⁴ and the removal of the 9-fluorenylmethoxycarbonyl (Fmoc) protecting group.¹⁵ The Belousov–Zhabotinsky (BZ) reaction (the best known oscillating chemical reaction) has autocatalysis as a core element,^{13, 16-17} as does a reaction based on the Kent ligation – a reaction that we have designed to oscillate.¹⁸

This work describes an autocatalytic, copper-catalyzed, azide-alkyne cycloaddition (CuAAC) reaction that uses the designed reduction of Cu(II) to Cu(I) to generate

1
2
3 autocatalysis. We can view the reaction as an autocatalytic cycle driven by the formation of a
4
5 ligand that promotes the reduction of Cu(II) to Cu(I) – where Cu(I) is the catalytic metal ion.
6
7 This autocatalytic organic reaction has the potential to be applied to a broad range of
8
9 substrates, and represents a potentially general mechanism to use in the design of
10
11 autocatalytic cycles.
12
13

14
15 Autoamplification and autocatalysis have been suggested as processes that contribute
16
17 to the solution of two core problems in considerations of the origin of life – that is “dilution”
18
19 and “mixtures”.¹⁹⁻²⁰ Although Eschenmoser, Sutherland, De Duve, Breslow, Wächtershäuser,
20
21 Morowitz, and many others have famously demonstrated how simple, plausible prebiotic
22
23 molecules (*e.g.*, cyanide, formaldehyde, formamide, sulfur dioxide, hydrogen sulfide, carbon
24
25 dioxide, others) can convert, usually, under *carefully* controlled laboratory conditions, into
26
27 the more complex molecules that make up metabolism (or fragments of them),^{2, 21-28} it
28
29 remains unclear how, or if, dilute solutions containing complex mixtures of these, and other,
30
31 compounds would do so. One possible solution to these problems is for reactions to occur in
32
33 enclosed or dimensionally constrained spaces (including, but not restricted to, liposomes or
34
35 vesicles, water droplets in oil, cracks in rocks, evaporating ponds, freezing water) or adsorbed
36
37 on surfaces.²⁹⁻³² A second solution to the problem of dilution/mixtures is autocatalysis and
38
39 autoamplification. Autoamplifying reactions – by providing very efficient conversion of
40
41 specific reactants to specific products – might provide one mechanism for generating high
42
43 local concentrations of these products. Autocatalysis, thus, might provide a route to increase
44
45 the availability of particular molecules (or sets of molecules) important for the emergence of
46
47 life.^{1, 33-37}
48
49
50
51
52
53

54 Multi-reaction systems that make up metabolism³⁸ do not ordinarily use direct
55
56 autocatalysis – that is, processes in which a catalytic entity catalyzes its own production.
57
58 Instead, complex autocatalytic cycles usually require multiple reactions to support
59
60

1
2
3 autoamplification.^{1-2, 18, 39-40} Acid-catalyzed hydrolysis of esters,⁴¹ formation of trypsin from
4 trypsinogen,⁴² autophosphorylation of protein kinase CK2,⁴³ and oxidation of oxalic acid by
5 permanganate are examples of direct autocatalysis.⁴⁴ The reverse Krebs cycle,^{40, 45} blood
6
7 coagulation cascade,⁴⁶ thiol autocatalytic reaction,¹⁸ and formose reaction are examples of
8
9 autocatalytic cycles.²
10
11
12
13

14
15 Although the subject of autoamplification/catalysis has been a subject of core interest
16
17 in chemistry, it has proved very difficult to design new autocatalytic cycles from organic
18
19 reactions. Despite the extraordinary versatility of organic chemistry, autocatalytic reactions
20
21 are surprisingly rare, and almost all have been discovered by accident.^{2-3, 9, 47} The literature on
22
23 autocatalytic reactions directly relevant to the one we have developed here is large, but not
24
25 predictive (at least so far) of new reactions.¹ Template-directed reactions, which were
26
27 pioneered by von Kiedrowski and Rebek,⁴⁸⁻⁵¹ are an exception. These reactions are designed
28
29 largely based on the rules of molecular recognition. They suffer, however, from product
30
31 inhibition and small (usually less than an order of magnitude) difference in rates of templated
32
33 and random reaction pathways, and from the structural complexity of the starting material.⁵²
34
35 Zubarev et. al, in search for prebiotic precursors to the citric acid cycle, used computational
36
37 approaches to propose plausible autocatalytic cycles in the chemistry of carboxylic acids.^{40,}
38
39
40
41
42
43
44
45
46
47
48
49
50
51
52
53
54
55
56
57
58
59
60

53 Our group recently designed a simple autocatalytic cycle based on chemistry of organic
thiols,¹⁸ and Otto and coworkers developed, after initial incidental discovery,
mechanochemical autocatalysis in assemblies of cyclic disulfides.⁵⁴

Early work by Finn⁵⁵, Fokin⁵⁶, Binder⁵⁷, and Hardy⁵⁸ suggested that the cycloaddition
step of Cu(I)-catalyzed click reactions can be autocatalytic. Finn⁵⁵ and Fokin⁵⁶ noticed that
tris-(triazolylmethyl)amines form Cu(I) complexes that are more reactive catalysts for
cycloaddition, and, therefore, suggested that the formation of *tris*-(triazolylmethyl)amines
from *tris*-(alkynylmethyl)amines proceeds autocatalytically. Although the kinetics of this

1
2
3 autocatalysis has not been characterized, Binder reported a CuAAC-based polymerization
4
5 that might also have proceeded autocatalytically, and Hardy demonstrated that a CuAAC
6
7 reaction can promote the self-replication of vesicles.⁵⁸ These examples, which begin from
8
9 catalytically active Cu(I) compounds, however, describe only modest rate enhancements (less
10
11 than an order of magnitude) over the course of the reactions.
12
13

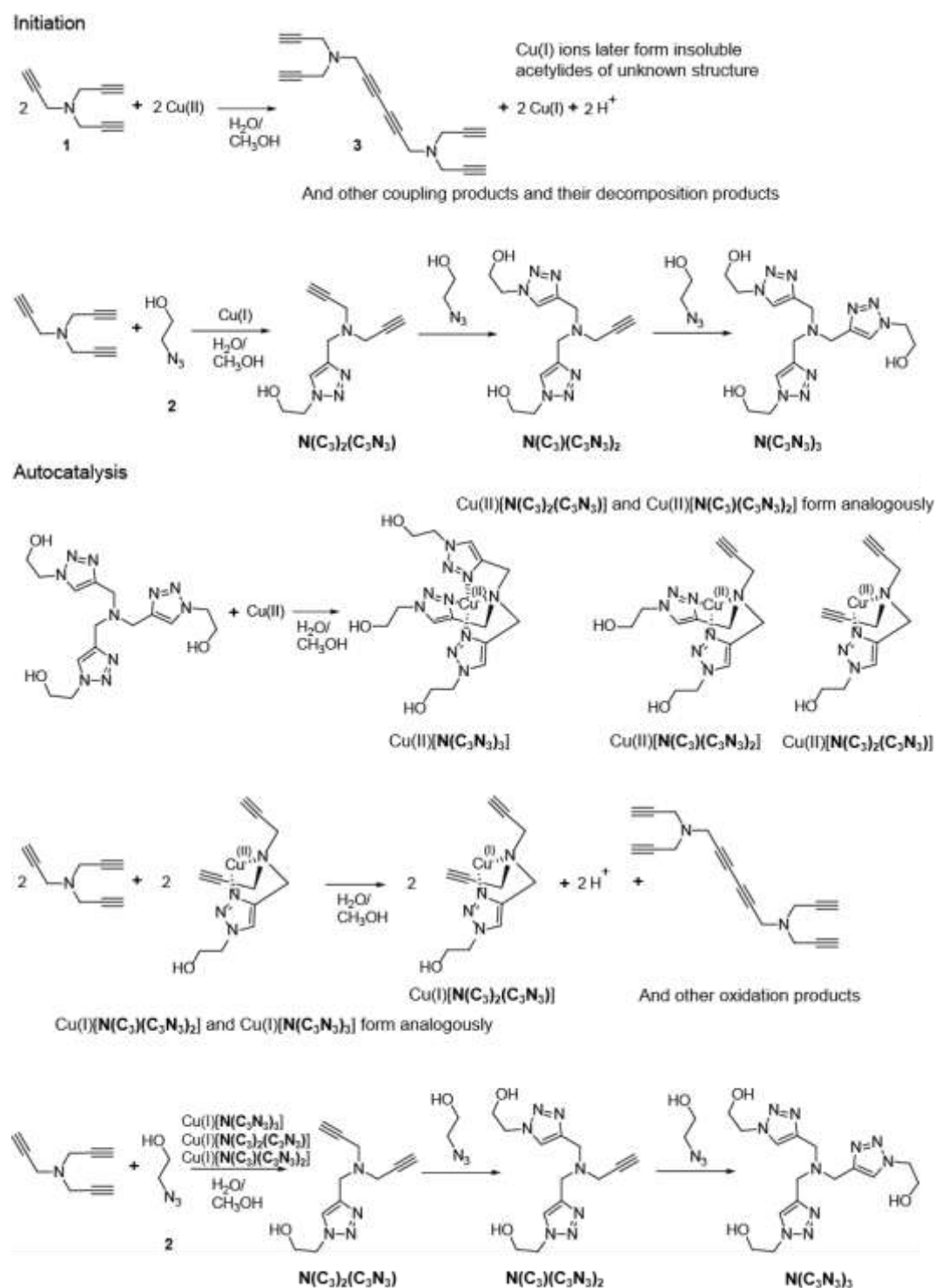
14
15 Our motivation for examining an autocatalytic copper-catalyzed click reaction, based
16
17 on the reduction of an inactive Cu(II) starting material to a catalytically active Cu(I) species,
18
19 was: i) Fokin⁵⁶ noted that *tris*-(triazolylmethyl)amine ligands appeared to stabilize Cu(I) from
20
21 disproportionation and increased the redox potential of Cu(I)/Cu(II) by nearly 300 mV. ii)
22
23 Zhu⁵⁹ observed that the CuAAC reaction proceeds with Cu(OAc)₂ in the absence of any
24
25 added reducing agent, and that the addition of 2 mol % of *tris*-(triazolylmethyl)amine ligands
26
27 increased the rate of the reaction. He suggested that: “*tris*-(triazolylmethyl)amine ligands may
28
29 increase the thermodynamic driving force for the reduction of Cu(II) during the induction
30
31 period to rapidly produce a highly catalytic Cu(I) species for the AAC reactions.”⁵⁹
32
33
34

35
36 The focus of this manuscript is on the participation of multiple reactions (reaction
37
38 networks) to generate a strong autocatalytic rate enhancement, which is an important kinetic
39
40 parameter for generating dynamic behaviours, such as oscillations and multi-stability, and for
41
42 creating conditions for chemical evolution.
43

44 **Results and Discussion**

45
46 We hypothesized that we could design an autocatalytic reaction with an initial reaction rate
47
48 that is negligible, thereby creating a larger difference between the initial and final rates of the
49
50 reaction by using – as a starting material – a water-soluble and catalytically inactive Cu(II)
51
52 salt (CuSO₄). To increase the concentration of the catalytic species, the triazole formed in this
53
54 reaction must be a ligand that promotes the reduction of Cu(II) to Cu(I), where Cu(I) is
55
56 required to form the active catalyst, which is likely a dynamic ensemble of multi-nuclear
57
58
59
60

Cu(I) species. Scheme 1 outlines the major features of the system of reactions we have examined.



Scheme 1. A simplified scheme describing the reactions that are involved in the autocatalytic formation of *tris*-(hydroxyethyltriazolymethyl)amine (**N(C₃N₃)₃**) *bis*-(hydroxyethyltriazolymethyl)propargylamine (**N(C₃)(N₃C₃)₂**) and (hydroxyethyltriazolymethyl)dipropargylamine (**N(C₃)(N₃C₃)₂**) from tripropargylamine (**1**) and 2-azidoethanol (**2**), in the presence of CuSO₄. The scheme uses the conversion of **1** to **3** to illustrate one plausible route for the initial reduction of Cu(II) to Cu(I), and does not consider alternative products from the oxidative coupling of **1**, or the nature of the Cu(I) species in the initiation step. The abbreviations we use for the compounds (*e.g.*, **N(C₃N₃)₃**) are indicated in bold-face text on the figure.

Kinetic Studies of the Reaction of Tripropargylamine with 2-Azidoethanol in the Presence of CuSO₄

We tested our hypothesis by allowing tripropargylamine (**1**) to react with 2-azidoethanol (**2**) and CuSO₄, in a water:methanol mixture (9:4; v:v) and monitored the reaction by ¹H-NMR spectroscopy. We performed this reaction by adding a solution of **1** (109 mM) in CD₃OD to a solution of **2** (309 mM) and CuSO₄ (43 mM) in D₂O, at room temperature (Fig. 1a). The low concentrations of reactants, compared to previous studies⁵⁵⁻⁵⁶, allowed us to overcome issues with product inhibition⁶² and to characterize the kinetics of the reaction in detail. Simple visual observation of the reaction showed an initially pale blue, almost clear, solution containing hydrated Cu(II) ions, which remained unchanged for about 20 minutes, before the solution became more opaque and – after approximately 50 minutes – changed to a dark blue color – a color typical of Cu(II) triazole complexes (Fig. 1c). This apparent incubation period, followed by a relatively sudden change of color (associated with the formation of Cu(II) triazole complexes), suggested that the reaction between **1**, **2**, and CuSO₄ has an autocatalytic character.

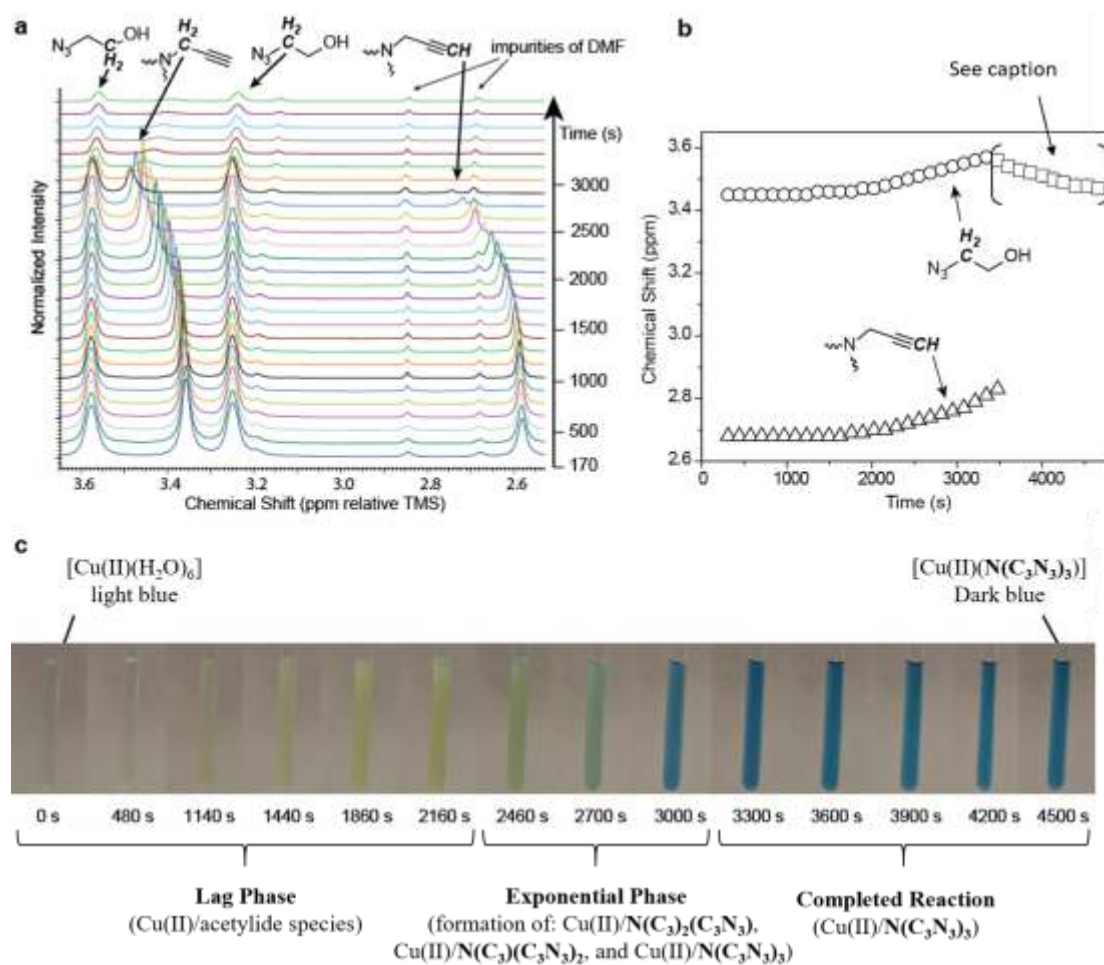


Figure 1. The time course of the reaction between tripropargylamine (**1**), 2-azidoethanol (**2**), and CuSO₄. Concentrations were estimated by integrating the alkyne proton against a *tert*-butanol internal standard. **a**) ¹H NMR spectra showing the disappearance of the proton signals of **1** and **2** over time. **b**) Plot of the chemical shifts of **1** during the first 3300 s of the reaction. After 3300 s, the alkyne protons (~ 2.6 ppm) disappear, and the propargylic protons (~ 3.4 ppm) change (bracketed region); this change indicates the formation of a small amount of a new species (□, whose structure we have not defined). **c**) Images of an NMR tube containing the reaction mixture at different times. Standard reaction conditions were **1** (109 mM), **2** (309 mM), and CuSO₄ (43 mM) in a mixture of D₂O/CD₃OD (9:4, v:v) at 25 °C.

Monitoring a reaction by NMR is often impractical in the presence of paramagnetic Cu(II) ions. Fortunately, however, the NMR signals of **1** and **2**, though slightly broad, were

1
2
3 sufficiently sharp for quantitative spectroscopy, and could be accurately integrated against an
4
5 internal standard of *tert*-butanol. The reaction products, *mono*-, *bis*- and *tris*-
6
7 (triazolylmethyl)amines, however, were not visible in the NMR spectrum when Cu(II) ions
8
9 were present.
10

11
12 To examine the kinetics of the reaction, we followed the disappearance of the alkyne
13
14 proton of **1**, at 2.6 ppm (Fig. 1a). We used this proton to monitor the progress of the reaction,
15
16 because it appears in a clear region of the NMR spectrum and H-D exchange was negligible
17
18 during an hour at pH 4.7 (which corresponds to the pH of the initial reaction mixture, see
19
20 supporting information for details). The kinetic profile of the reaction resembled that of a
21
22 typical autocatalytic reaction, with a lag phase, an exponential phase, and a saturation phase
23
24 (Fig. 2a). The exponential phase was accompanied by a shift (of only partly identified origin)
25
26 in the resonance frequency of the protons of **1** (Fig. 1b), which correlated with the change in
27
28 color of the solution to dark blue. We determined the final composition of the reaction
29
30 mixture by reducing all remaining Cu(II) to $[\text{Cu(I)(CN)}_x]^{(x-1)-}$ with an excess of potassium
31
32 cyanide⁶³⁻⁶⁴, and analyzing the mixture by ¹H NMR spectroscopy. The final product of the
33
34 reaction was the tripodal ligand *tris*-(2-hydroxyethyltriazolylmethyl)amine (which we
35
36 abbreviate as **N(C₃N₃)₃**), which formed in 85% yield (as determined by ¹H-NMR); the
37
38 methylene signal adjacent to the amine was integrated relative to an internal *tert*-butanol
39
40 standard.
41
42
43
44
45

46
47 If a reaction is autocatalytic, then addition of the autocatalyst to the reaction will
48
49 shorten its lag phase. We performed an NMR kinetics experiment, identical in form to the
50
51 one described above, but with the addition of **N(C₃N₃)₃** (1 mol % relative to **1**) and observed
52
53 a decrease in the duration of the lag phase, by a factor of three (Fig. 2a).
54
55
56
57
58
59
60

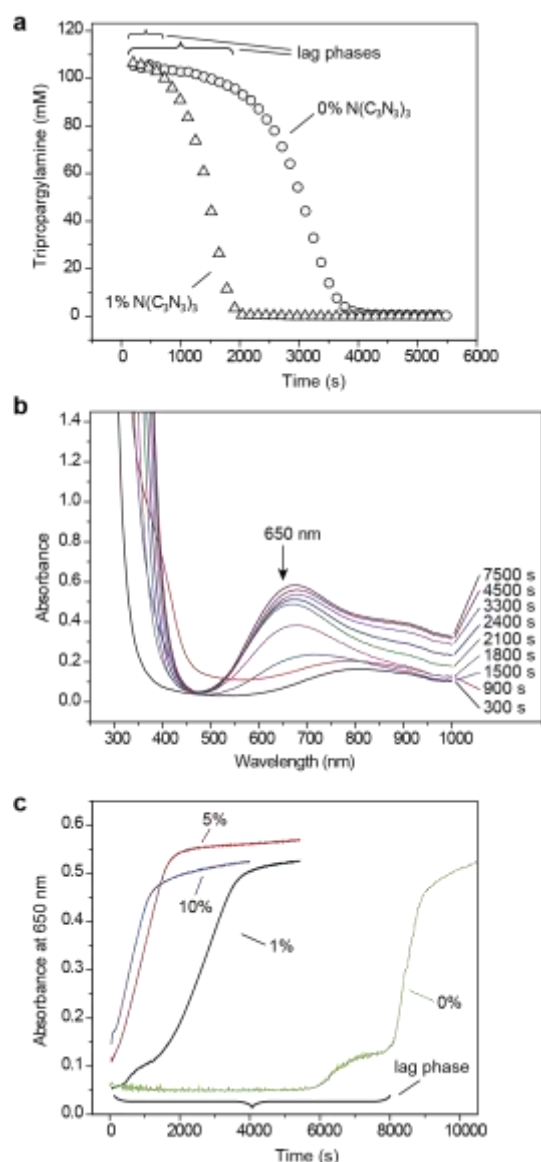


Figure 2. Experiments showing elimination of the lag period with the addition of an autocatalyst in the reaction between **1** (109 mM), **2** (309 mM), and $CuSO_4$ (43 mM). **a)** Plot showing the disappearance of the alkyne proton of **1** (at 2.6 ppm) over time, as determined by 1H NMR. The numbers above the traces show the mol% of *tris*-(2-hydroxyethyltriazolylmethyl)-amine ($N(C_3N_3)_3$) added relative to **1**. All reactions were performed in a mixture of D_2O/CD_3OD (9:4, v:v) at 25 °C, in an NMR tube, and the concentration of tripropargylamine was calculated by integrating the alkyne proton against a *tert*-butanol internal standard. **b)** UV-Vis absorption spectra at various time points during the reaction with 1 mol% of autocatalyst (the mixture of complexes of *mono*-, *bis*- and *tris*-

1
2
3 (triazolylmethyl)amines with copper) added relative to **1**, in a H₂O/CH₃OH (9:4, v:v) mixture
4
5 at 25 °C. Copper complexes of triazolylmethylamines absorb at 650 nm. c) UV-Vis analysis
6
7 of the reaction, using the same conditions as in **b**, performed by measuring the absorption at
8
9 650 nm. The numbers above the traces show the approximate mol% of the autocatalyst (the
10
11 mixture of complexes of *mono*-, *bis*- and *tris*-(triazolylmethyl)amines with copper from a
12
13 reaction that had previously reached completion) relative to **1**.
14
15
16
17
18

19
20 We also tested the reaction in a H₂O:CH₃OH (9:4, v:v) mixture by monitoring the
21
22 change in absorption at 650 nm (Fig. 2b), because Cu(II)-triazolylmethylamines complexes
23
24 absorb light more strongly at this wavelength than unbound Cu(II) (*i.e.*, the aqua complex)
25
26 (Fig. S2). Unexpectedly, in the reaction without any added autocatalyst, there was no
27
28 detectable reaction within the first 6000 s, and autocatalysis began only after 7000 s (~2
29
30 hours) (Fig. 2c; details of this difference in rate are discussed in a following section). The
31
32 addition of 1 mol % (relative to **1**) of the autocatalyst – the mixture of complexes of *mono*-,
33
34 *bis*- and *tris*-(triazolylmethyl)amines with copper from the previously complete reaction –
35
36 shortened the lag phase to 1800 s, and the addition of 5 mol % or 10 mol % of the
37
38 autocatalyst completely eliminated the lag phase (Fig. 2c).
39
40
41

42
43 During the reaction of **1** (109 mM), **2** (309 mM), and CuSO₄ (43 mM) in a
44
45 H₂O:CH₃OH (9:4, v:v) mixture, the pH of the solution increased from 4.7 to 6.2. To test
46
47 whether this increase of 1.5 pH units contributed to autocatalysis we ran the reaction in
48
49 acetate buffer (340 mM), but under otherwise identical reaction conditions. The buffered
50
51 reaction gave similar kinetics to that of the unbuffered reaction, suggesting that the change in
52
53 pH does not contribute strongly to autocatalysis (Fig. S3).
54
55

56 ***Propagation of an Autocatalytic Reaction Front.*** Autocatalytic reactions form autocatalytic
57
58 fronts when they take place without mixing.⁶⁵ The observation of an autocatalytic front
59
60

1
2
3 provides additional support for autocatalysis, as opposed to other mechanisms for delayed
4
5 activation. For instance, simple CuAAC reactions accelerated by *tris*-triazolyl ligands can
6
7 have observable lag phases⁶⁶. Because the catalytic species in CuAAC reactions are multi-
8
9 nuclear, and under most circumstances only a fraction of the total copper present is a part of
10
11 the operational catalyst, the required evolution of catalyst speciation may result in an
12
13 observable lag phase. We demonstrated that the autocatalytic CuAAC reaction formed an
14
15 observable lag phase. We demonstrated that the autocatalytic CuAAC reaction formed an
16
17 autocatalytic reaction front by performing the reaction in a layer of 1 % agarose gel (1 mm
18
19 thick) in H₂O:CH₃OH (9:4, v:v), loaded with **1** (125 mM), **2** (309 mM), and CuSO₄ (84 mM).
20
21 We initiated autocatalysis by adding a small (~0.1 mm) crystal of ascorbic acid (which
22
23 rapidly reduces Cu(II) to Cu(I)) (Fig. 3a and supplementary video). Initially, the agarose gel
24
25 appeared clear, with weak blue coloring. When the ascorbic acid was added, the area in
26
27 contact with the crystal turned yellow, because Cu(II) was reduced to Cu(I) (which, in the
28
29 presence of alkynes, forms polynuclear Cu(I) acetylide complexes that are yellow). The area
30
31 in contact with Cu(I) subsequently underwent the CuAAC reaction, and as triazolyl ligands
32
33 were produced, the gel turned to the dark blue color associated with Cu(II)/triazolyl
34
35 complexes. The area closest to the ascorbic acid crystal used to initiate the reaction remained
36
37 yellow because Cu(II) was being continuously reduced to Cu(I). The autocatalytic front
38
39 propagated radially with constant velocity (as illustrated by the time/space plot, Fig. 3b) at a
40
41 rate of 0.0325 ± 0.0010 mm/min. Propagation of the reaction front continued for 4 hours,
42
43 with a final radius of 10 mm.
44
45
46
47
48

49 Two characteristics of the autocatalytic CuAAC reaction described here make it
50
51 suitable for the study of dynamic phenomena in reaction-diffusion systems: (i) a low rate of
52
53 spontaneous activation; and (ii) an easy detection by color change. We note that organic
54
55 autocatalytic reactions (*i.e.* autocatalytic reaction of thiols and template-directed reactions)¹⁸.

56
57
58 ⁵¹ usually have rates of spontaneous activation that prevent prolonged observation of an
59
60

1
2
3 autocatalytic front. For example, an autocatalytic reaction front driven by the template-
4 directed cycloaddition of a nitron to an alkene propagated only for about 20 min before the
5 reaction spontaneously activated in bulk.⁵² By contrast, for the system described in this paper,
6
7
8
9
10
11
12
13
14
15
16
17
18
19
20
21
22
23
24
25
26
27
28
29
30
31
32
33
34
35
36
37
38
39
40
41
42
43
44
45
46
47
48
49
50
51
52
53
54
55
56
57
58
59
60

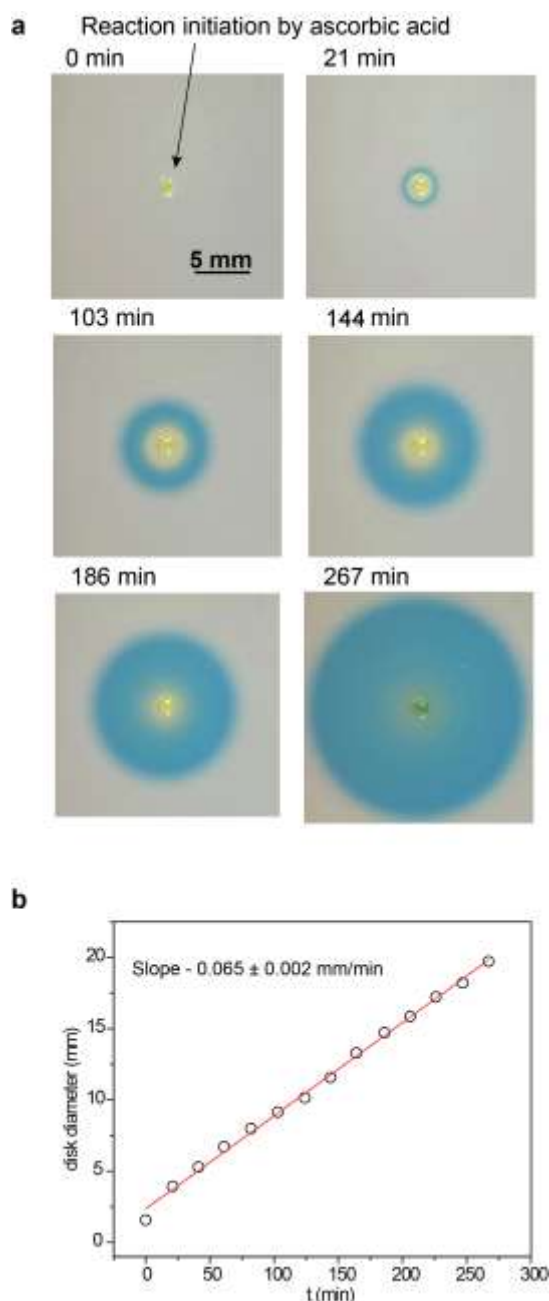


Figure 3. Reaction front driven by the autocatalytic copper catalyzed azide-alkyne cycloaddition. **a)** Photographs of the reaction propagating in 1 mm thick agarose gel loaded

1
2
3 with **1** (125 mM), azidoethanol (320 mM), and CuSO₄ (84 mM). We initiated the reaction at
4
5 the central point in the gel using a crystal of ascorbic acid. The yellow color comes from the
6
7 reduced Cu(I) species, the blue color comes from the Cu(II) complex with N(C₃N₃)₃ (Cu(II)
8
9 N(C₃N₃)₃) and indicates progress of the reaction. **b)** Graph that shows that the reaction front
10
11 propagates with constant velocity.
12
13
14

15 16 17 *Mechanism of the Reaction of Tripropargylamine With 2-Azidoethanol in the Presence of* 18 19 *CuSO₄.*

20
21 **Initiation of the Reaction.** Our initial hypothesis was that autocatalysis would require the
22
23 addition of a reducing reagent to convert Cu(II) to Cu(I). In fact, this reduction proceeded in
24
25 the presence of only **1** and **2**: no additional reducing agent was required. Because the
26
27 reduction of Cu(II) to Cu(I) by alkynes is a well-known reaction, and is the basis for the
28
29 Eglinton coupling,⁶⁷ we propose that **1** (either as an alkyne or a tertiary amine) acts as a
30
31 reducing agent in the reaction. To test this hypothesis, we mixed **1** (109 mM) and CuSO₄ (43
32
33 mM) in D₂O:CD₃OD in the absence of azide **2**. The yellow precipitate expected for a Cu(I)
34
35 acetylide formed within an hour. X-ray photoelectron spectroscopic (XPS) data confirmed
36
37 the presence of Cu(I), carbon, and nitrogen in this precipitate (Fig. 4a; Fig. S4).
38
39
40
41

42
43 To determine which functional group of **1** (the alkyne or the amine) acts as the
44
45 reducing agent, we examined two model reactions: (i) We allowed propargyl alcohol (500
46
47 mM) to react with CuSO₄ (43 mM) in acetate buffer (200 mM, pH 4.7) at 60 °C for 2 min,
48
49 and (ii) we allowed triethylamine (110 mM) to react with CuSO₄ (43 mM) in acetate buffer
50
51 (200 mM, pH 4.7) at 60 °C for 2 min. The reaction with propargyl alcohol resulted in the
52
53 reduction of Cu(II) to Cu(I), and formation of a yellow precipitate of Cu(I) acetylide, while
54
55 no reaction was observed with triethylamine. ESI-MS data from the reaction of **1**, **2**, and
56
57 CuSO₄ in H₂O:CH₃OH showed the presence of butadiyne **3** in the reaction mixture (M+Na⁺
58
59
60

1
2
3 283.1). We therefore infer that the reduction of Cu(II) to Cu(I) by the alkyne functionality of
4
5 **1** is likely the initiation step for the cycloaddition between the azide and alkyne. To support
6
7 this proposal, we demonstrated that increasing the starting concentration of **1** decreased the
8
9 duration of the lag phase (Fig. 4b). We note, however, that the reduction in the lag phase may
10
11 be partially influenced by the increased concentration of the tertiary amine, which could be
12
13 functioning to depolymerize unreactive and highly-aggregated Cu(I) acetylides⁶².
14
15

16 17 ***Catalytic Properties of Cu(I) Complexes with Tris-triazolylmethylamines***

18
19 To investigate the contribution of *tris*-triazolylmethylamine ligands on the
20
21 acceleration of the Cu(I)-catalyzed cycloaddition reaction, we performed a control
22
23 experiment in which Cu(I) was added at the start of the reaction, and was maintained in the
24
25 reduced state by the presence of a 2x excess (relative to the concentration of CuSO₄) of
26
27 ascorbic acid (supporting information Fig. S5). Reactions initiated with Cu(I) at 43 mM
28
29 proceeded at rates that were too large to be monitored by NMR. To decrease the rate of the
30
31 reaction to a rate that is compatible with NMR analysis, and especially to monitor the initial
32
33 stages of the reaction, we decreased the concentration of copper to 2 mM. Because Cu(I) was
34
35 present at the beginning of the reaction, we saw no lag phase. We did, however, observe a
36
37 slight (approximately 2x) increase in rate during the initial stages of the reaction; the
38
39 observation is compatible with autocatalysis. Because the initial concentration of Cu(I) was
40
41 lower, the speciation of Cu(I) (which may have a significant impact on the rate of the
42
43 cycloaddition⁶⁸) will have been different, and thus the rate (and change in rate over time) is
44
45 not necessarily directly comparable with our other experiments. Nevertheless, this increase in
46
47 rate, although small compared to our systems that use Cu(II) as a precursor, is probably
48
49 analogous to the rate enhancement reported by Fokin,^{56, 62} and is comparable to that reported
50
51 by Binder.⁵⁷
52
53
54
55
56
57
58
59
60

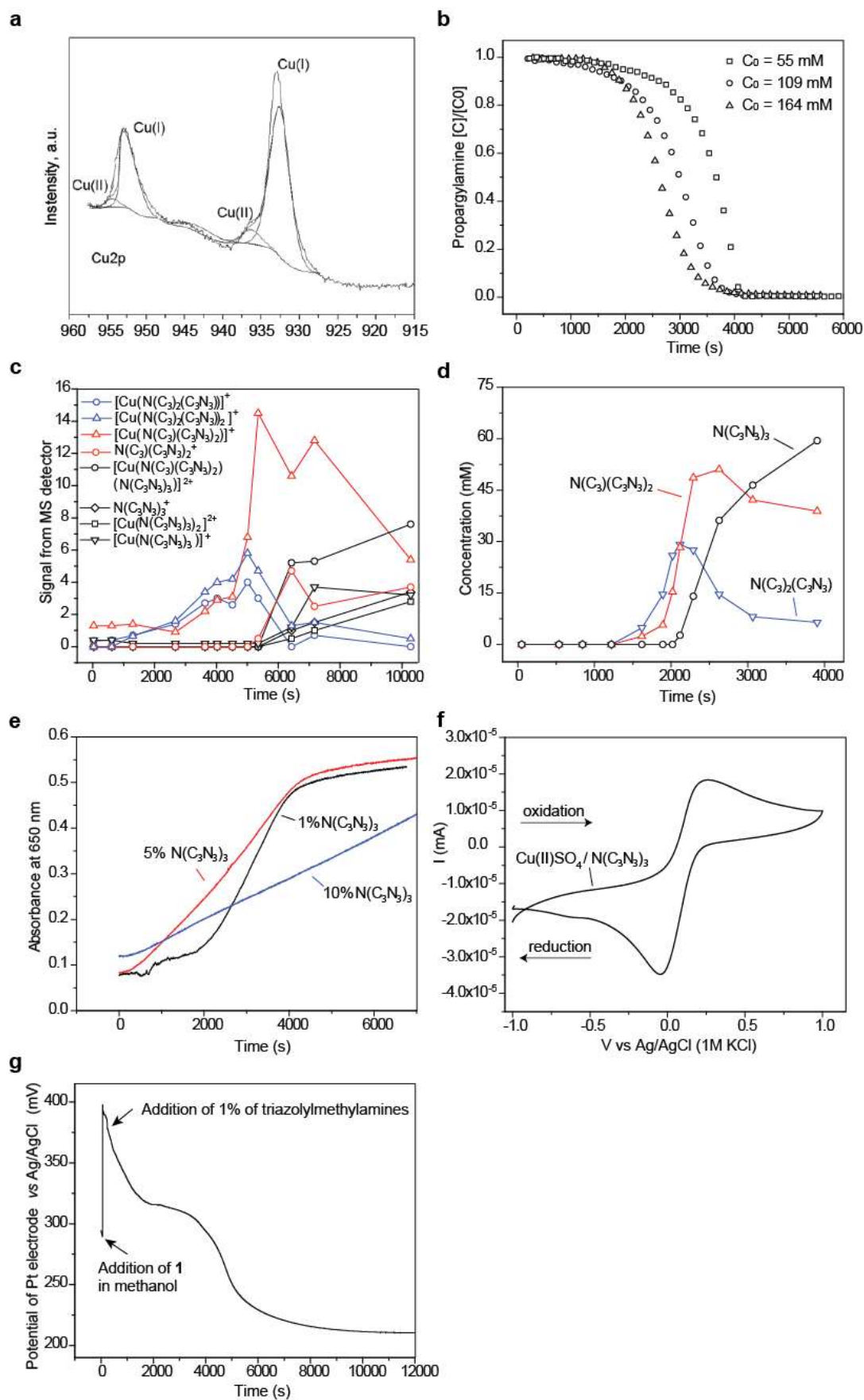


Figure 4. Mechanistic studies of the reaction between **1**, **2**, and CuSO₄. **a)** XPS data showing the presence of Cu(I) in the precipitate formed in the reaction of **1** (109 mM) and CuSO₄ (43 mM) in D₂O/CD₃OD (9:4, v:v) mixture. **b)** ¹H NMR kinetic experiments for the reaction between **1**, **2** (309 mM), and CuSO₄ (43 mM) in a D₂O/CD₃OD (9:4 v:v) mixture at 25 °C, starting from different amounts of **1**. The concentration of tripropargylamine was calculated by integrating the alkyne proton against a *tert*-butanol internal standard. **c)** Changes in intensity of ESI-MS signals of some triazole species during the autocatalytic CuAAC reaction. The reaction was carried out under the same conditions as the experiment shown in panel **d**. **d)** Change in concentrations of N(C₃)₂(C₃N₃), N(C₃)(C₃N₃)₂, and N(C₃N₃) in the reaction of **1** (109 mM), **2** (309 mM), and CuSO₄ (43 mM) determined by NMR measurements. Samples were removed from the reaction and quenched by addition to 2 weight% aqueous solutions of KCN. **e)** UV-vis analysis of reactions with different starting concentrations of N(C₃N₃)₃. The reaction contained **1** (109 mM), **2** (309 mM), and CuSO₄ (43 mM) in H₂O/CH₃OH (9:4 v:v) mixture at 25 °C. **f)** Cyclic voltammogram (scan rate 100 mV/s) of CuSO₄ (5 mM), Na₂SO₄ (50 mM), and N(C₃N₃)₃ (10 mM) in H₂O/CH₃OH (9:4 v:v). **g)** The change in potential of a Pt wire electrode vs a Ag|AgCl reference electrode (1.0 M KCl as reference solution) during the reaction of **1** (109 mM), **2** (309 mM), and CuSO₄ (43 mM) in a H₂O/CH₃OH (9:4 v:v) mixture at 25 °C. The reaction was initiated by 1 mol % of triazolylmethylamines.

The Role of Intermediate Cycloaddition Products. The simplified sequence of reactions summarized in Scheme 1 proposes sequential formation of *mono*-, *bis*-, and *tris*-(2-hydroxyethyltriazolylmethyl)amines. We investigated the roles of these species in autocatalysis. First, we used ESI-MS to monitor the reaction (see experimental section for details), and observed that (2-hydroxyethyltriazolylmethyl)dipropargylamine (N(C₃)₂(C₃N₃)),

1
2
3 and *bis*-(2-hydroxyethyltriazolylmethyl)propargylamine ($\text{N}(\text{C}_3)(\text{C}_3\text{N}_3)_2$) were the major
4 species formed during the initial stages of the reaction (*i.e.*, during the lag phase),
5
6
7 $\text{N}(\text{C}_3)(\text{C}_3\text{N}_3)_2$ was the major species formed during the exponential phase, and *tris*-(2-
8 hydroxyethyltriazolylmethyl)amine ($\text{N}(\text{C}_3\text{N}_3)_3$) was formed in significant quantities only near
9 the end of the reaction (once almost all of the tripropargylamine had been consumed; Fig.
10
11
12
13
14
15 4c). Second, we measured the kinetics of the reaction by NMR spectroscopy by collecting
16
17 100- μL samples, quenching them in KCN solution (2 weight% in $\text{D}_2\text{O}:\text{CD}_3\text{OD}$), and
18
19 measuring their NMR spectra (Fig. S6). KCN quenches the reaction by converting all Cu(II)
20
21 to $[\text{Cu}(\text{I})(\text{CN})_x]^{(x-1)-}$, which is not an active catalyst for cycloaddition. This system also
22
23 permits recording of ^1H NMR spectra, where $\text{N}(\text{C}_3)_2(\text{C}_3\text{N}_3)$, $\text{N}(\text{C}_3)(\text{C}_3\text{N}_3)_2$, and $\text{N}(\text{C}_3\text{N}_3)_3$ are
24
25 visible and resolvable. The results show that no triazole compounds are formed (above the
26
27 detection limit of NMR spectroscopy: about 1 mM) until 800 s (rate $< 1.25 \cdot 10^{-3}$ mM/s), and
28
29 that the maximum rate of formation of triazoles, at around 2000 s, is about 0.5 mM/s (Fig. 4d,
30
31
32 Fig S9). Thus, we observed a rate enhancement of more than 400x, which explains the
33
34 prolonged propagation of the autocatalytic front without spontaneous reaction outside of the
35
36 reaction front. Consistent with the MS data, $\text{N}(\text{C}_3)(\text{C}_3\text{N}_3)_2$ was the major species formed
37
38 during the exponential phase (Fig. 4d). This result might be, at least partially, a consequence
39
40 of product inhibition by bidentate chelation of two $\text{N}(\text{C}_3)(\text{C}_3\text{N}_3)_2$ ligands to Cu(I),⁶²
41
42 effectively trapping the active Cu(I) catalyst in a stable, inactive, form and briefly isolating
43
44 $\text{N}(\text{C}_3)(\text{C}_3\text{N}_3)_2$ from further reaction.
45
46
47
48

49 Both the MS and NMR experiments suggest that the formation of $\text{N}(\text{C}_3\text{N}_3)_3$ from
50
51 $\text{N}(\text{C}_3)(\text{C}_3\text{N}_3)_2$ is not cooperative, since $\text{N}(\text{C}_3\text{N}_3)_3$ is not formed in the earlier stages of the
52
53 reaction. The NMR data, however, suggested that the formation of $\text{N}(\text{C}_3)(\text{C}_3\text{N}_3)_2$ from
54
55 $\text{N}(\text{C}_3)_2(\text{C}_3\text{N}_3)$, is, to some extent, cooperative, since $\text{N}(\text{C}_3)_2(\text{C}_3\text{N}_3)$ did not accumulate in the
56
57 mixture and was quickly converted to $\text{N}(\text{C}_3)(\text{C}_3\text{N}_3)_2$.
58
59
60

1
2
3 To understand the roles of the $\text{N}(\text{C}_3\text{N}_3)_2(\text{C}_3\text{N}_3)$, $\text{N}(\text{C}_3)(\text{C}_3\text{N}_3)_2$, and $\text{N}(\text{C}_3\text{N}_3)_3$ in the
4 autocatalytic process, we studied the effect of adding them to the initial reaction mixture on
5 the kinetics of this reaction (Fig. 4e and supporting information Fig. S7). Adding a small
6 amount of $\text{N}(\text{C}_3\text{N}_3)_3$ (1 mol % relative to **1**) resulted in a kinetic curve that is effectively
7 indistinguishable from that obtained by adding 1 mol % (relative to **1**) of the mixture from
8 the completed reaction (*i.e.*, a mixture of $\text{N}(\text{C}_3)_2(\text{C}_3\text{N}_3)$, $\text{N}(\text{C}_3)(\text{C}_3\text{N}_3)_2$, $\text{N}(\text{C}_3\text{N}_3)_3$, and their
9 copper complexes). Adding either 5 mol % or 10 mol % of $\text{N}(\text{C}_3\text{N}_3)_3$ eliminated the lag
10 phase, but also decreased the maximum slope of the kinetic curve. When 10 mol % of
11 $\text{N}(\text{C}_3)_2(\text{C}_3\text{N}_3)$ or $\text{N}(\text{C}_3)(\text{C}_3\text{N}_3)_2$ was added to the reaction, the lag phase (which included the
12 interval from 0 - 4000 s for $\text{N}(\text{C}_3)_2(\text{C}_3\text{N}_3)$, and from 0 - 1000 s for $\text{N}(\text{C}_3)(\text{C}_3\text{N}_3)_2$; Fig. S7)
13 was not completely eliminated, although the slopes of the kinetic curves were higher than in
14 the experiment with 1 mol % of $\text{N}(\text{C}_3\text{N}_3)_3$. This observation suggested that $\text{N}(\text{C}_3\text{N}_3)_3$ is the
15 most active of these three species in accelerating the reduction of Cu(II) to Cu(I), although
16 $\text{N}(\text{C}_3)(\text{C}_3\text{N}_3)_2$ might play a more important role in catalyzing the CuAAC reaction. We note
17 here, however, that the exact mechanism for the reduction of Cu(II) to Cu(I), and the nature
18 of the species involved, are not known.

19
20
21
22
23
24
25
26
27
28
29
30
31
32
33
34
35
36
37
38
39
40 **Electrochemical studies.** We hypothesized that triazolylmethylamines stabilize Cu(I)
41 against disproportionation in water/methanol mixtures. Cu(I) ions disproportionate in water,
42 or water/methanol mixtures, to Cu(II) and Cu(0)⁶⁹. As a consequence of the tendency for
43 Cu(I) to disproportionate, the cyclic voltammogram (CV) obtained from CuSO₄ (5 mM) in a
44 mixture of H₂O:CH₃OH (9:4, v:v) gave two oxidation and reduction peaks (Fig. S8). The CV
45 of CuSO₄ (5 mM) and $\text{N}(\text{C}_3\text{N}_3)_3$ (10 mM), in a mixture of H₂O:CH₃OH (9:4, v:v), however,
46 gave only one peak (Fig. 4f), corresponding to the reduction of Cu(II) to Cu(I). The ligand,
47 $\text{N}(\text{C}_3\text{N}_3)_3$, pushes the redox potential of the reduction of Cu(I)/Cu(0) to negative values, to
48 the extent that we do not observe this peak within the 2 V potential window. This shift in the
49
50
51
52
53
54
55
56
57
58
59
60

1
2
3 $E^{\circ}_{\text{Cu(I)/Cu(0)}}$ makes the disproportionation of Cu(I) unfavorable ($E_{\text{disproportionation}} = E_{\text{Cu(I)/Cu(0)}} -$
4 $E_{\text{Cu(II)/Cu(I)}}$), and stabilizes Cu(I) in the complex with $\text{N}(\text{C}_3\text{N}_3)_3$. This stabilization of the
5
6 catalytically active Cu(I) ions in solution facilitates the cycloaddition reaction.
7
8
9

10 To monitor the redox reactions taking place during the autocatalytic reaction, we
11 recorded the open-circuit potential of the solution. We monitored the potential of a Pt wire
12 (relative to a Ag/AgCl reference electrode) during the reaction between **1** (109 mM), **2** (309
13 mM), and CuSO_4 (43 mM), in a $\text{H}_2\text{O}:\text{CH}_3\text{OH}$ mixture. Figure 4g shows the resulting
14 potential curve, which has four characteristic features: (i) an initial spike in potential,
15 immediately after the addition of **1**; (ii) an 80 mV drop in potential after the addition of 1%
16 triazolylmethylamines (500 – 2000 s); (iii) a period of approximately constant potential (2000
17 – 4000 s); and (iv) a 100 mV drop in potential starting at 4000 s. The potential drop at 4000 s
18 correlated with a color change from pale to dark blue. Although unambiguous interpretation
19 of open circuit potential measurements is difficult, the second drop in potential (4500 s)
20 might plausibly originate from an increase in the concentration of Cu(I), caused by the
21 chemical reduction of Cu(II) during the autocatalytic process.
22
23
24
25
26
27
28
29
30
31
32
33
34
35
36

37 ***Inverse Solvent Kinetic Isotope Effect.*** We observed (based on the duration of the lag
38 phase) an apparent inverse solvent kinetic isotope effect (KIE) in the reaction between **1**, **2**,
39 and CuSO_4 (that is, the lag phase ended earlier in $\text{D}_2\text{O}:\text{MeOD}$ (9:4, v:v) than in $\text{H}_2\text{O}:\text{MeOH}$
40 (9:4, v:v)). The lag phase ends at around 1500 s (~25 min) in $\text{D}_2\text{O}/\text{MeOD}$ (Fig. 2b), and after
41 7000 s (~116 min) in $\text{H}_2\text{O}/\text{MeOH}$, under otherwise identical reaction conditions (Fig. 2b).
42 Because we believe that the lag phase is a consequence of the slow reduction of Cu(II) to
43 Cu(I), the observed solvent kinetic isotope effect likely involves the alkyne-mediated
44 reduction of Cu(II) to Cu(I). The details of the mechanism and intermediate species of the
45 reduction of Cu(II) to Cu(I) by terminal alkynes are complex, and are still under considerable
46 debate⁷⁰ (as are the details of the mechanism and intermediate species of the CuAAC
47
48
49
50
51
52
53
54
55
56
57
58
59
60

1
2
3 reaction⁷¹). The processes that are believed to be involved, however, (hybridization changes,
4 reductive elimination, and/or transition metal C-H activation) are chemical processes often
5 associated with KIEs⁷².
6
7
8
9

10 We hypothesized that, in deuterated solvent and in the presence of copper, the alkyne
11 protons of **1** may exchange with deuterium from D₂O and/or MeOD, and that the deuterated
12 product **1-d₃** (*i.e.*, tripropargylamine with its three alkyne protons replaced with deuterium)
13 may be the origin of the observed inverse KIE. We thus ran the reaction between **1-d₃**, **2**, and
14 CuSO₄ in a mixture of H₂O:MeOH (9:4, v:v), and monitored the reaction by UV/Vis
15 spectroscopy, at 650 nm (Fig. 5). As a control, we also ran the reaction between **1-d₃**, **2**, and
16 CuSO₄ in a mixture of D₂O:MeOD (9:4, v:v).
17
18
19
20
21
22
23
24
25

26 Figure 5 shows the reaction progress of four different reactions, run under the same
27 reaction conditions: 1) **1-d₃**, **2**, and CuSO₄ in a mixture of H₂O:MeOH (9:4, v:v); 2) **1-d₃**, **2**,
28 and CuSO₄ in a mixture of D₂O:MeOD (9:4, v:v); 3) **1**, **2**, and CuSO₄ in a mixture of
29 H₂O:MeOH (9:4, v:v); 4) **1**, **2**, and CuSO₄ in a mixture of D₂O:MeOD (9:4, v:v).
30
31
32
33
34

35 If **1-d₃** were causing the observed inverse KIE, the duration of the lag phase of the
36 reaction involving **1-d₃** and H₂O/MeOH would resemble that observed in the reaction of **1**
37 and D₂O/MeOD. Figure 5, however, shows that the lag phase for the reaction with **1-d₃** in
38 H₂O/MeOH was even longer than that using **1** in H₂O/MeOH, ending after ~11000s (183
39 min). This observed normal KIE supports the involvement of the alkyne proton in the lag
40 phase (reduction of Cu(II) to Cu(I)), but also indicates that it is not the origin of the observed
41 inverse KIE. Furthermore, the control reaction between **1-d₃**, **2**, and CuSO₄ in a mixture of
42 D₂O:MeOD (9:4, v:v), had a longer lag phase than that of **1** in D₂O/MeOD. Thus, while the
43 alkyne displays a normal KIE, and is involved in the lag phase, the observed inverse solvent
44 KIE is not affected by the alkyne proton. The idea that these two KIEs act independently is
45
46
47
48
49
50
51
52
53
54
55
56
57
58
59
60

supported by the effect of isotopic substitution of the alkyne (**1**-d₃) on the duration of the lag phase, which was roughly the same for both solvent systems.

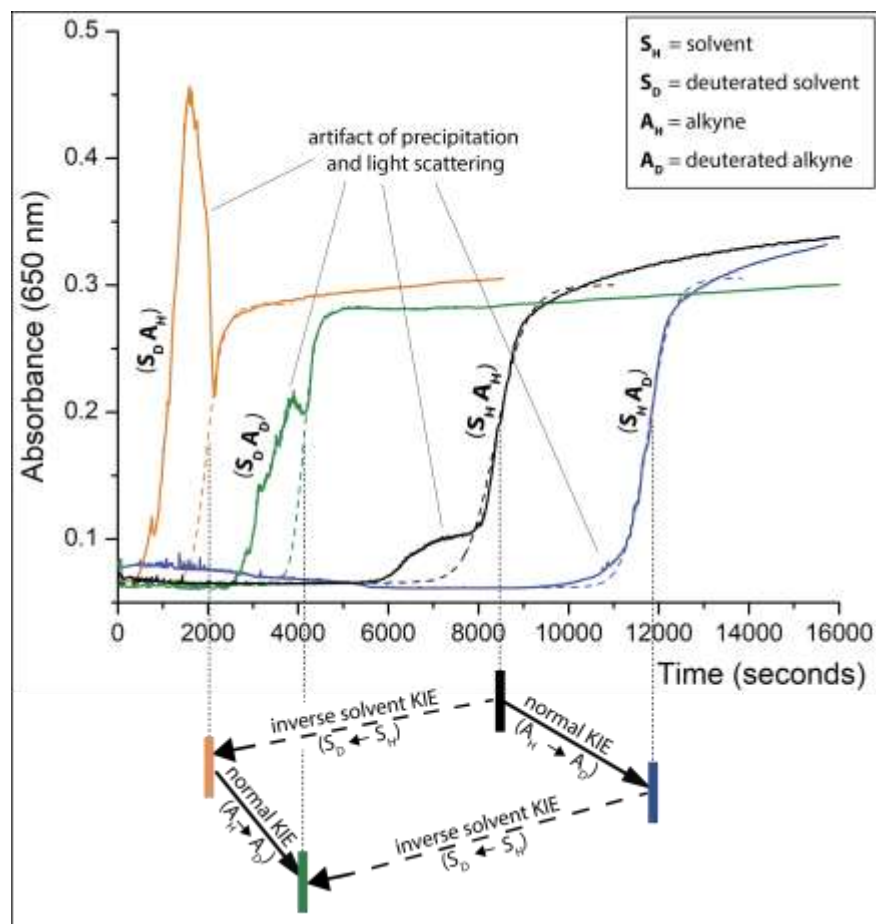


Figure 5. Top: reaction progress monitored by UV/Vis spectroscopy, at 650 nm, of four different reactions. In all forms, the starting concentrations were: **1** or **1**-d₃ (109 mM), **2** (309 mM), and CuSO₄ (43 mM) in a mixture of H₂O:MeOH or D₂O; MeOD (9:4, v:v). The dashed lines are sigmoidal fits to the data, omitting the region containing the artifact of precipitation and light scattering. Bottom: Representation of how the two kinetic isotope effects (KIEs) plausibly and approximately independently influence the lag phase of these four reactions. The position of the colored bars corresponds to the approximate duration of the lag phase on the x-axis.

1
2
3 Figure 5 indicates that these reactions show a spike in absorbance as the lag phase
4 ends. This absorbance peak corresponds to the formation of precipitates, which we expect are
5 insoluble Cu(I) intermediates. The intensity of this absorbance peak (and thus the degree of
6 precipitation) also correlates with the duration of the lag phase (reactions with shorter lag
7 phases have larger absorbance peaks). We attribute this observation to the fact that shorter lag
8 phases have more rapid formation of Cu(I) intermediates, which thus accumulate in larger
9 concentrations (and thus precipitate to larger extents).

10
11
12
13
14
15
16
17
18
19 Given that the inverse solvent KIE is not affected by the alkyne proton but is still
20 involved in the reduction of Cu(II), we suspected that D₂O and/or MeOD may influence the
21 reduction potential of the Cu(II)/N(C₃N₃)₃ complex. We did not, however, see a change in the
22 cyclic voltammogram (scan rate 100 mV/s) of CuSO₄ (5 mM), Na₂SO₄ (50 mM), and
23 N(C₃N₃)₃ (10 mM) in D₂O/CH₃OD (9:4; v:v), as compared to that in H₂O/CH₃OH (9:4; v:v)
24 (Fig. 4f). We can thus only speculate that these deuterated solvents influence the rate of
25 reduction of Cu(II) to Cu(I) through an isotope-dependent solvation effect that reduces the
26 activation free energy of electron transfer.⁷³ We have thus not identified the origin of the
27 negative KIE at this time. Since this mechanistic feature—while interesting—is secondary to
28 the focus of the work, we leave it unresolved.

29
30
31
32
33
34
35
36
37
38
39
40
41
42 **Summary of the Mechanism.** We summarize our current inferences concerning the
43 mechanism of the autocatalytic CuAAC reaction as follows: The reaction starts with an
44 initial, slow, reduction of hydrated Cu(II) to Cu(I), where an alkyne serves as the reducing
45 agent. The reduction of Cu(II) to Cu(I) by the acetylenic group of N(CH₂C≡CH)₃ (**1**), leads to
46 the initial Cu(I) complexes that are catalytically active in the cycloaddition. The products of
47 the initial and subsequent cycloadditions—N(C₃)₂(C₃N₃), N(C₃)(C₃N₃)₂, and N(C₃N₃)₃
48 (Scheme I)—form coordination complexes with Cu(I) and Cu(II). Uncoordinated Cu(I) is
49 unstable in water/methanol solutions and disproportionates. Here, the triazolyl amine ligands
50
51
52
53
54
55
56
57
58
59
60

1
2
3 form stable and soluble complexes with Cu(I), which maintain copper in its catalytically
4 active oxidation state, Cu(I), in solution. The formation of $\text{N}(\text{C}_3)_2(\text{C}_3\text{N}_3)$, $\text{N}(\text{C}_3)(\text{C}_3\text{N}_3)_2$, and
5 $\text{N}(\text{C}_3\text{N}_3)_3$ also accelerate the reduction of Cu(II) to Cu(I), although the exact reasons for this
6 acceleration are unclear, and might involve intermediates in the CuAAC reaction.
7
8
9
10

11
12 Thus, formation of the Cu(I) species—the catalytically active species in the click
13 (cycloaddition) reaction—is promoted by the formation of ligands that are the product of that
14 reaction. The reaction cycle is autocatalytic because the production, and stability in solution,
15 of Cu(I) is promoted by the aminotriazolyl ligands, and production of the aminotriazolyl
16 ligands is accelerated by Cu(I) (Scheme 2). The Cu(I) species that are formed in the reduction
17 process might, however, be initially catalytically inactive and require extra steps to rearrange
18 into catalytically active complexes. An additional contribution to autocatalysis, although
19 probably a less important one, comes from the increased activity of Cu(I) in the CuAAC
20 reaction when it is complexed with an aminotriazolyl ligand. As the CuAAC reaction
21 (catalyzed by Cu(I)) progresses, more aminotriazolyl ligands are produced. The
22 aminotriazolyl ligands coordinate Cu(I) (in addition to Cu(II)) to form a more reactive Cu(I)
23 catalyst, which in turn accelerates the rate of formation of the aminotriazolyl ligands.
24
25
26
27
28
29
30
31
32
33
34
35
36
37
38
39

40 Based on this reaction profile, we have developed a numerical model, involving six
41 simplified reactions, to describe the proposed mechanism (see supporting information for
42 details). The numerical solution of these equations shows kinetics that resemble the
43 experimental data (supporting information, Fig. S9). This type of modeling shows that a
44 plausible kinetic scheme (with adjustable rate constants) can model the observed data
45 adequately. As with all similar weakly constrained models, “compatibility” is not “proof”,
46 but the goodness of fit of the simulated data—using physically plausible values of rate
47 constants—provides further support for the general scheme proposed.
48
49
50
51
52
53
54
55
56
57
58
59
60

component has only a weak influence on the kinetics of the reaction, and that the reaction can tolerate a variety of substituted azides.

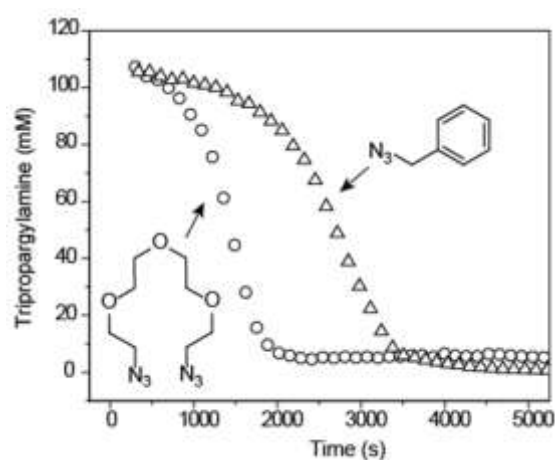
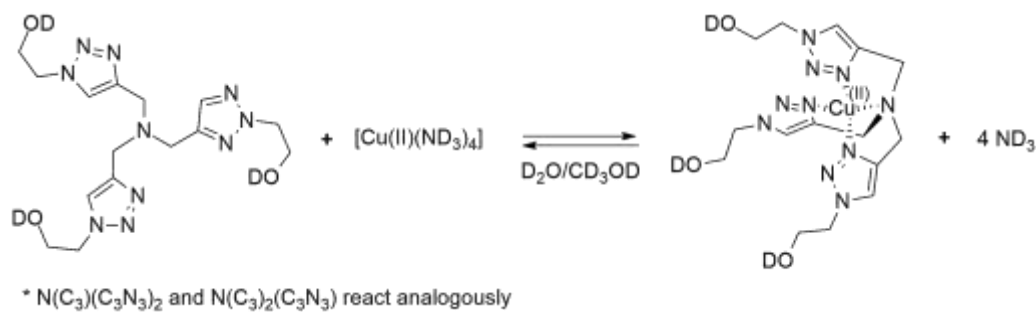


Figure 6. Scope of the autocatalytic CuAAC reaction. ^1H NMR kinetics experiments for the reaction between **1** (109 mM), CuSO_4 (43 mM), and tetraethylene glycol diazide (**4**, 150 mM) or benzylazide (**5**, 260 mM). The experiment with **4** was conducted in a $\text{D}_2\text{O}/\text{CD}_3\text{OD}$ (9:4, v:v) mixture at 25 °C. The experiment with **5** was conducted in pure CD_3OD . The concentration of alkyne was calculated by integrating the alkyne proton against a *tert*-butanol internal standard.

We also tested the reaction of **2** (327 mM) with propargylamine (309 mM) and CuSO_4 (43 mM) in a water/methanol (9:4, v:v) mixture. The reaction displays sigmoidal kinetics, but the formation of precipitates, and the combination of copper speciation, disproportionation of Cu(I) complexes, and depolymerization of insoluble Cu polyacetylenes, makes an unambiguous interpretation of this sigmoidal kinetic curve challenging (Fig S10 and supplementary discussion).

Displacing Ammonia From Cu(II) ions.

A possible extension of the autocatalytic cycle (Scheme 2) is the displacement of a ligand that binds to Cu(II) (such as ammonia) by the triazolylmethylamines formed in the reaction (Scheme 3). The release of a free ligand opens a new path to couple autocatalysis to independent chemical reactions.



14 **Scheme 3.** Substitution of ammonia from Cu(II) ammonia complex by $N(C_3N_3)_3$ ligand.

15
16
17
18
19 We ran the reaction of **1**, **2**, and $CuSO_4$ in the presence of ammonia (240 mM) and
20 ammonium chloride (430 mM), and monitored the reaction by 1H NMR. The disappearance
21 of **1** followed an approximately sigmoidal curve, characteristic of an autocatalytic reaction
22 (Fig. 7). The formation of precipitates during intermediate stages of the reaction may be the
23 cause of the deviation of the course of the reaction from the expected sigmoid. When the
24 reaction was complete, the solution was pale yellow, which is in contrast to the bright blue
25 color of reactions without ammonia. The most plausible explanation for this difference in
26 color is a faster reduction of Cu(II) aminotriazolyl complexes in the presence of ammonia,
27 perhaps as a result of the increased pH of the solution. Reduction of Cu(II), thus, happens
28 faster than cycloaddition, and all copper is reduced to yellow Cu(I) complexes. When
29 exposed to air, the color of the complete reaction mixture changes back to blue. This
30 experiment demonstrated that we can extend the scope of the autocatalytic CuAAC reaction
31 to reactions that involve complexes of Cu(II). This experiment also provided further evidence
32 that autocatalysis is not a consequence of an increase in pH during the reaction, because the
33 reaction remains autocatalytic when performed in an ammonia/ammonium chloride buffer.
34
35
36
37
38
39
40
41
42
43
44
45
46
47
48
49
50
51
52
53
54
55
56
57
58
59
60

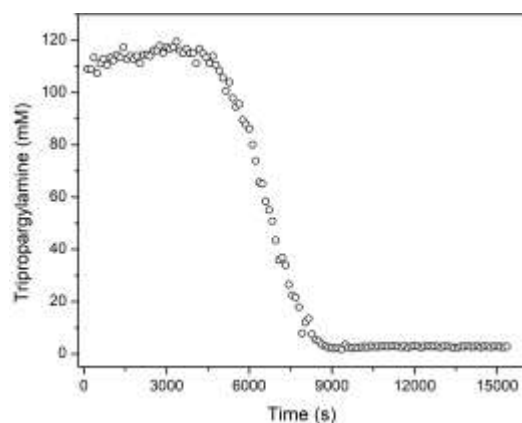


Figure 7. ^1H NMR kinetic experiments for the reaction between propargylamine (109 mM), azidoethanol (309 mM), CuSO_4 (43 mM), NH_3 (240 mM), and NH_4Cl (430 mM).

Experiments were conducted in $\text{D}_2\text{O}/\text{CD}_3\text{OD}$ (9:4 v:v) mixture at 25 °C. The concentration of tripropargylamine was calculated by integrating the alkyne proton against a *tert*-butanol internal standard.

Conclusions

This work describes an autocatalytic system where coupling the CuAAC reaction and the reduction of Cu(II) to Cu(I) affords a large rate enhancements over the course of the reaction. We consider this system of reactions as prototypical of autocatalytic cycles. In this example, a classical catalytic cycle (the CuAAC reaction) is coupled to a process (the reduction of Cu(II) to Cu(I)) that generates an extra molecule of the catalyst – a process that “amplifies” the number of molecules of catalyst (in principle, exponentially) and that underlies the mechanism of all autocatalytic reactions. This system is driven by the catalytic formation of a product that, by acting as a ligand, enhances the production and activity of the catalyst. This characteristic of the product(s) is achieved by (i) the formation of a nucleophilic triazole ring from a non-nucleophilic azido group, and (ii) the formation of a chelate ligand, from a monodentate ligand. Specifically, the organic azide group from azidoethanol (which does not bind strongly to copper ions) converts to a triazole (which does

1
2
3 coordinate strongly to copper ions) and a monodentate tripropargylamine converts to a
4
5 tetradentate triazolylmethylamine (which bind tightly to Cu(I) and Cu(II) ions).
6
7

8 The autocatalytic CuAAC reaction is compatible with a range of substrates, and can,
9
10 in principle, generate polymeric/oligomeric products. We illustrated two subtypes of the
11
12 autocatalytic cycle (See Scheme S1, supporting information): (i) the product ligand forms the
13
14 active catalyst from a solvated metal ion; (ii) the product ligand forms a complex from a
15
16 metal ion containing an ancillary ligand which is released upon complexation.
17
18

19 This reaction will aid in the development and understanding of chemical reaction
20
21 networks. This, and other work examining mechanisms of autocatalysis, may also help to
22
23 form a better picture of the processes that led to the emergence of life on earth, because
24
25 similar processes (kinetically, although certainly—in this case—not in molecular detail)
26
27 might generate autocatalysis in mixtures of molecules (for example, alkynes and nitriles, or
28
29 metal ions bound to peptides) that may have been important for the origin of life.^{74 75-76}
30
31
32
33
34

35 **Associated Content**

36 *Supporting Information*

37
38 Experimental details of syntheses and kinetics experiments.

39
40 Details of the kinetic model describing autocatalysis.

41
42 Supplementary video of the propagating autocatalytic front.

43
44 The Supporting Information is available free of charge on the ACS Publications website.

45 **Author Information**

46 *Corresponding Author*

47
48 * E-mail: gwhitesides@gmwgroup.harvard.edu

49 *Present Addresses*

50
51 ‡ *Department of Organic Chemistry, Weizmann Institute of Science, Rehovot 76100, Israel.*

52
53 † *SCAMT Laboratory, ITMO University, St. Petersburg 197101, Russian Federation.*

Acknowledgements

This work was supported by an award (290364) from the Simons Foundations. LB acknowledges fellowship support from NSERC Canada. RC acknowledges the Harvard REU program under NSF award DMR-1420570.

References

1. Bissette, A. J.; Fletcher, S. P., *Angew. Chem. Int. Ed.* **2013**, *52*, 12800-12826.
2. Breslow, R., *Tetrahedron Lett.* **1959**, 22-26.
3. Boutlerow, A. M., *Comptes Rendus Chimie* **1869**, *53*, 145-147.
4. James, T. H.; Mees, C. E. K., *The Theory of the photographic process*. 4th ed.; Macmillan: New York, 1977; p xvii, 714 p.
5. Ichimura, K., *Chem. Rec.* **2002**, *2*, 46-55.
6. Kruger, S.; Revuru, S.; Higgins, C.; Gibbons, S.; Freedman, D. A.; Yueh, W.; Younkin, T. R.; Brainard, R. L., *J. Am. Chem. Soc.* **2009**, *131*, 9862.
7. Kruger, S. A.; Higgins, C.; Cardincau, B.; Younkin, T. R.; Brainard, R. L., *Chem. Mater.* **2010**, *22*, 5609-5616.
8. Mallory, G. O.; Hajdu, J. B.; American Electroplaters and Surface Finishers Society., *Electroless plating : fundamentals and applications*. The Society: Orlando, Fla., 1990; p viii, 539 p.
9. Soai, K.; Shibata, T.; Morioka, H.; Choji, K., *Nature* **1995**, *378*, 767-768.
10. Soai, K.; Kawasaki, T., *Top. Curr. Chem.* **2008**, *284*, 1-33.
11. Soai, K.; Kawasaki, T., *Chirality* **2006**, *18*, 469-478.
12. Blackmond, D. G., J., *Proc. Natl. Acad. Sci. U.S.A.* **2004**, *101*, 5732.
13. Kovacs, K.; McIlwaine, R. E.; Scott, S. K.; Taylor, A. F., *J. Phys. Chem. A* **2007**, *111*, 549-551.
14. Kovacs, K.; McIlwaine, R. E.; Scott, S. K.; Taylor, A. F., *Phys. Chem. Chem. Phys.* **2007**, *9*, 3711-3716.
15. Arimitsu, K.; Ichimura, K., *J. Mater. Chem.* **2004**, *14*, 336-343.
16. Belousov, B. P., *Sbornik Referatov po Radiatsionni Meditsine* **1958**, 145.
17. Gyorgyi, L.; Turanyi, T.; Field, R. J., *J. Phys. Chem., US* **1990**, *94*, 7162-7170.
18. Semenov, S. N.; Kraft, L. J.; Ainla, A.; Zhao, M.; Baghbanzadeh, M.; Campbell, C. E.; Kang, K.; Fox, J. M.; Whitesides, G. M., *Nature* **2016**, *537*, 656-660.
19. Hordijk, W.; Hein, J.; Steel, M., *Entropy-Switz.* **2010**, *12*, 1733-1742.
20. Eigen, M.; Schuster, P., *Naturwissenschaften* **1978**, *65*, 7-41.
21. Patel, B. H.; Percivalle, C.; Ritson, D. J.; Duffy, C. D.; Sutherland, J. D., *Nat. Chem.* **2015**, *7*, 301-307.
22. Eschenmoser, A., *Tetrahedron* **2007**, *63*, 12821-12844.
23. De Duve, C., *Singularities: Landmarks on the Pathways of Life*. Cambridge University Press: Cambridge, UK, 2005.
24. Ricardo, A.; Carrigan, M. A.; Olcott, A. N.; Benner, S. A., *Science* **2004**, *303*, 196.
25. Smith, E.; Morowitz, H. J., J., *Proc. Natl. Acad. Sci. U.S.A.* **2004**, *101*, 13168-13173.
26. Huber, C.; Wächtershäuser, G., *Science* **1997**, *276*, 245-247.
27. Cody, G. D.; Boctor, N. Z.; Filley, T. R.; Hazen, R. M.; Scott, J. H.; Sharma, A.; Yoder, H. S., *Science* **2000**, *289*, 1337-1340.

28. Butch, C.; Cope, E. D.; Pollet, P.; Gelbaum, L.; Krishnamurthy, R.; Liotta, C. L., *J. Am. Chem. Soc.* **2013**, *135*, 13440-13445.
29. Morowitz, H. J.; Heinz, B.; Deamer, D. W., *Orig. Life Evol. Biospheres* **1988**, *18*, 281-287.
30. Monnard, P.-A.; Kanavarioti, A.; Deamer, D. W., *J. Am. Chem. Soc.* **2003**, *125*, 13734-13740.
31. Burcar, B.; Pasek, M.; Gull, M.; Cafferty, B. J.; Velasco, F.; Hud, N. V.; Menor-Salván, C., *Angew. Chem. Int. Ed.* **2016**, *55*, 13249-13253.
32. Hazen, R. M.; Sverjensky, D. A., *Cold Spring Harb. Perspect. Biol.* **2010**, *2*.
33. Pross, A., *Orig. Life Evol. Biospheres* **2005**, *35*, 151-166.
34. Kauffman, S. A., *At Home in the Universe: The Search for Laws of Self-organization and Complexity*. Oxford University Press: 1995.
35. Eigen, M.; Schuster, P., *The Hypercycle: A Principle of Natural Self-Organization*. Springer Berlin Heidelberg: 1979.
36. Eschenmoser, A., *Angew. Chem. Int. Ed.* **2011**, *50*, 12412-12472.
37. Hordijk, W.; Steel, M., *Biosystems* **2017**, *152*, 1-10.
38. Barenholz, U.; Davidi, D.; Reznik, E.; Bar-On, Y.; Antonovsky, N.; Noor, E.; Milo, R., *Elife* **2017**, *6*.
39. Lincoln, T. A.; Joyce, G. F., *Science* **2009**, *323*, 1229-1232.
40. Zubarev, D. Y.; Rappoport, D.; Aspuru-Guzik, A., *Sci. Rep.-Uk* **2015**, *5*.
41. Xu, Y.; Chen, Q.; Zhao, Y. J.; Lv, J.; Li, Z. H.; Ma, X. B., *Ind. Eng. Chem. Res.* **2014**, *53*, 4207-4214.
42. Neurath, H.; Dreyer, W. J., *Discuss. Faraday Soc.* **1955**, 32-43.
43. Donella-Deana, A.; Cesaro, L.; Sarno, S.; Brunati, A. M.; Ruzzene, M.; Pinna, L. A., *Biochem. J.* **2001**, *357*, 563-567.
44. Launer, H. F., *J. Am. Chem. Soc.* **1932**, *54*, 2597-2610.
45. Morowitz, H. J.; Kostelnik, J. D.; Yang, J.; Cody, G. D., *Proc. Natl. Acad. Sci. U.S.A.* **2000**, *97*, 7704-7708.
46. Davie, E. W.; Fujikawa, K.; Kisiel, W., *Biochemistry-US* **1991**, *30*, 10363-10370.
47. Flegeau, E. F.; Bruneau, C.; Dixneuf, P. H.; Jutand, A., *J. Am. Chem. Soc.* **2011**, *133*, 10161-10170.
48. von Kiedrowski, G., *Angew. Chem. Int. Ed.* **1986**, *25*, 932-935.
49. Sievers, D.; von Kiedrowski, G., *Nature* **1994**, *369*, 221-224.
50. Tjivikua, T.; Ballester, P.; Rebek, J., *Abstr. Pap. Am. Chem. Soc.* **1990**, *199*, 46-Orgn.
51. Wintner, E. A.; Conn, M. M.; Rebek, J., *J. Am. Chem. Soc.* **1994**, *116*, 8877-8884.
52. Bottero, I.; Huck, J.; Kosikova, T.; Philp, D., *J. Am. Chem. Soc.* **2016**, *138*, 6723-6726.
53. Rappoport, D.; Galvin, C. J.; Zubarev, D. Y.; Aspuru-Guzik, A., *J. Chem. Theory Comput.* **2014**, *10*, 897-907.
54. Carnall, J. M. A.; Waudby, C. A.; Belenguer, A. M.; Stuart, M. C. A.; Peyralans, J. J. P.; Otto, S., *Science* **2010**, *327*, 1502-1506.
55. Chan, T. R.; Hilgraf, R.; Sharpless, K. B.; Fokin, V. V., *Org. Lett.* **2004**, *6*, 2853-2855.
56. Dohler, D.; Michael, P.; Binder, W. H., *Macromolecules* **2012**, *45*, 3335-3345.
57. Flory, P. J., *Principles of Polymer Chemistry*. Cornell University Press: 1953.
58. Hardy, M. D.; Yang, J.; Selimkhanov, J.; Cole, C. M.; Tsimring, L. S.; Devaraj, N. K., *Proc. Natl. Acad. Sci. U.S.A.* **2015**, *112*, 8187-8192.
59. Kuang, G.-C.; Michaels, H. A.; Simmons, J. T.; Clark, R. J.; Zhu, L., *J. Org. Chem.* **2010**, *75*, 6540-6548.
60. Flory, P. J., *Principles of Polymer Chemistry*. Cornell University Press: 1953.

- 1
2
3
4
5
6
7
8
9
10
11
12
13
14
15
16
17
18
19
20
21
22
23
24
25
26
27
28
29
30
31
32
33
34
35
36
37
38
39
40
41
42
43
44
45
46
47
48
49
50
51
52
53
54
55
56
57
58
59
60
61. Rostovtsev, V. V.; Green, L. G.; Fokin, V. V.; Sharpless, K. B., *Angew. Chem. Int. Ed.* **2002**, *41*, 2596.
 62. Rodionov, V. O.; Presolski, S. I.; Diaz, D. D.; Fokin, V. V.; Finn, M. G., *J. Am. Chem. Soc.* **2007**, *129*, 12705-12712.
 63. Parkash, R.; Zýka, J., *Microchem. J.* **1972**, *17*, 309-317.
 64. Roof, R. B., Jr; Larson, A. C.; Cromer, D. T., *Acta Crystallogr. B* **1968**, *24*, 269-273.
 65. Epstein, I. R.; Pojman, J. A., *An introduction to nonlinear chemical dynamics : oscillations, waves, patterns, and chaos*. Oxford University Press: New York, 1998; p xiv, 392 p.
 66. Rodionov, V. O.; Presolski, S. I.; Gardinier, S.; Lim, Y.-H.; Finn, M. G., *J. Am. Chem. Soc.* **2007**, *129*, 12696-12704.
 67. Eglinton, G.; Galbraith, A. R., *J. Chem. Soc.* **1959**, 889.
 68. Rodionov Valentin, O.; Fokin Valery, V.; Finn, M. G., *Angew. Chem. Int. Ed.* **2005**, *44*, 2210-2215.
 69. Rorabacher, D. B.; Schroeder, R. R., Electrochemistry of Copper. In *Encyclopedia of Electrochemistry*, John Wiley and Sons, Inc.: 2007; pp 992 - 1046.
 70. Zhang, G.; Yi, H.; Zhang, G.; Deng, Y.; Bai, R.; Zhang, H.; Miller, J. T.; Kropf, A. J.; Bunel, E. E.; Lei, A., *J. Am. Chem. Soc.* **2014**, *136*, 924-926.
 71. Jin, L.; Tolentino, D. R.; Melaimi, M.; Bertrand, G., *Sci. Adv.* **2015**, *1*.
 72. Gómez-Gallego, M.; Sierra, M. A., *Chem. Rev.* **2011**, *111*, 4857-4963.
 73. Farver, O.; Zhang, J.; Chi, Q.; Pecht, I.; Ulstrup, J., *Proc. Natl. Acad. Sci. U.S.A.* **2001**, *98*, 4426.
 74. Wachtershauser, G., *P Natl Acad Sci USA* **1990**, *87*, 200-204.
 75. Scintilla, S.; Bonfio, C.; Belmonte, L.; Forlin, M.; Rossetto, D.; Li, J. W.; Cowan, J. A.; Galliani, A.; Arnesano, F.; Assfalg, M.; Mansy, S. S., *Chem. Commun.* **2016**, *52*, 13456-13459.
 76. Beinert, H., *J. Biol. Inorg. Chem.* **2000**, *5*, 2-15.

ToC Image:

